J Fluoresc (2011) 21:11–15
DOI 10.1007/s10895-010-0683-4

ORIGINAL PAPER

Global Analysis of Dynamic Fluorescence Anisotropy by a Polarized Phasor Approach

Yanzhou Zhou · Long Wu · Qinruo Wang · Yonghua Wang

Received: 18 April 2010 / Accepted: 26 May 2010 / Published online: 8 June 2010

Abstract Recently, the graphical analysis of the fluorescence lifetime imaging using the phasor approach has been highlight, and a series of the reports have made it on the way for the applications by the nonprofessionals. In this paper, we put forward a similar theory validated by the experiments for the dynamic fluorescence anisotropy imaging. By subtracting the perpendicular component from the parallel one in the frequency-domain polarization measurement, we deduce a new analytical expression about the fluorescence joint time, and find that as much as the fluorophore is a single exponential decay and r_∞ is equal to zero, $^{\triangle}I(t)$ is a single exponential decay with the time constant X as well, and the center of its histograms is located on the semicircle in the polarized phasor plot. In the end, we conclude that the fluorescence joint time is the best parameter to weigh the fluorescence dynamics for the macromolecules.

Keyword Phasor plot · Fluorescence dynamic anisotropy · Fluorescence microscopy

Graphical representation of the fluorescence lifetime processing, referred to as phasor approach, polar plot or AB plot, has been proven to be a valuable tool to analysis single or multiple lifetime components from different molecule species [1–9]. In addition to the fluorescence lifetime, i.e., time-resolved fluorescence anisotropy with the nature of exponential decay arising from the rotational motion of fluorophores is particularly useful on the interpretation of the macromolecule rotation in the local environment and non-radiative energy transfer (FRET) among the molecules [10–14]. Because of the similarity and correlation between the fluorescence lifetime and dynamic anisotropy, the phasor approach can be updated to evaluate anisotropy quantitatively avoiding the fatal problems coming from the global fitting of exponential analysis and intensity interference [12, 15]. From the first principle, we may find that it succeeds the advantages of the phasor plot for the fluorescence lifetime analysis, such as the direct mapping between the selections of the phasor space and fluorescence intensity image makes the visual analysis of different photophysical processing accessible to the non professionals [7], and the approach is independent from the hardware configuration [7, 10, 12, 16]. In the section below, we first deduce the analytical formulae for the polarized phasor plot, then show the phasor histograms of the fluorescence joint time for the mixtures of the different concentrations between glycerol and rhodamine 6G experimentally.

Although the phasor approach is suitable for the quantitive analysis of dynamic anisotropy no matter whether the hardware configuration is based on the time-domain method or on the frequency-domain method [7, 10, 12, 16], in this paper, we take the measurement of the fluorescence anisotropy in the frequency-domain for example. The measurement of the fluorescence lifetime using frequency-domain method normally consists of a light source and detector, which are modulated using a single frequency, f_0. A series of images are collected while the phase is shifted by the equal step between the excitation source and detector, and Fourier transformed to recover modulation depth m and phase shift φ between the excitation and emission light. The lifetimes from the

Y. Zhou (✉) · L. Wu · Q. Wang · Y. Wang
Faculty of Automation, Guangdong University of Technology, Guangzhou, Guangdong 510006, People's Republic of China
e-mail: zhouyanzhou@hotmail.com

modulation depth m and phase shift φ may then be calculated, respectively [13],

$$\tau_m = \omega_o^{-1} \cdot \sqrt{\frac{1}{m^2} - 1},\ \tau_\varphi = \omega_o^{-1} \cdot \tan\,\varphi, \tag{1}$$

where $\omega_o = 2\pi\, f_0$. In order to avoid the complexity of the global nonlinear least square fitting, it is often convenient to present a transformation of the fluorescence lifetime as a phasor plot [1, 2, 5, 7, 8, 17, 18],

$$B = m \cdot \cos\varphi,\ A = m \cdot \sin\varphi. \tag{2}$$

For a single exponential decay, (B, A) should be mapped to be a point on the semicircle in the phasor space. If a mixture of the multiple nointeractive fluorophores is concerned, A and B are related to the fluorescence lifetime and fractions of each species by [2, 3, 7, 9]

$$A = \sum_{i=1}^{n} \frac{f_i \cdot \omega_0 \cdot \tau_{\varphi \cdot i}}{1 + \omega_0^2 \cdot \tau_{\varphi \cdot i}^2},\ B = \sum_{i=1}^{n} \frac{f_i}{1 + \omega_0^2 \cdot \tau_{m \cdot i}^2}, \tag{3}$$

where f_i is the intensity weighted fractional contribution of the ith component [7]. A single exponential decay is represented by a point on the semicircle in the phasor plot. On this semicircle, a phasor corresponding to a very short lifetime is close to the point (1,0), while a phasor corresponding to a very long lifetime will be close to the point (0,0).

Suppose the fluorescence comes from two nointeractive fluorophores with single exponential decays, respectively, the fluorescence lifetime may be depicted by the points in the phasor space using linear interpolation among (B_i, A_i) and f_i ; however, if one of the fluorescence components is exponential rising, the mapping point in the phasor space should be constructed using the linear extrapolation of (B_i, A_i) and f_i, which is possibly located outside the semicircle. The latter case widely exists in the photophysics, such as photo bleaching, energy transfer [5], and dynamic fluorescence anisotropy [12], etc.

The method described from Eqs. 1–3 may be extended to the dynamic fluorescence anisotropy measurement by providing a polarized excitation source and collecting two sets of images. The first set is collected with an excitation polarizer oriented parallel to the analyzing polarizer and the second set with it oriented perpendicular. Therefore, the light intensity $I(t)$ may then be calculated [13],

$$I(t) = I_{\|}(t) + 2 \cdot I_{\perp}(t) = I_0 \cdot \exp(-t/\tau), \tag{4}$$

where I_0 represents the light intensity at 'zero time', and the subscripts II, $\perp$ refer to the orientation of the analyzing polarizer parallel and perpendicular, respectively.

The time-resolved anisotropy $r(t)$ with an exponential tail can also be presented as the function of parallel and perpendicular components [13],

$$\begin{aligned} r(t) &= (r_0 - r_\infty) \cdot \exp(-t/\theta) + r_\infty, \\ r(t) &= \tfrac{I_{\mathrm{II}}(t) - I_\perp(t)}{I_{\mathrm{II}}(t) + 2I_\perp(t)} = \tfrac{I_{\mathrm{II}}(t) - I_\perp(t)}{I(t)}. \end{aligned} \tag{5}$$

where r_0 is the fundamental anisotropy, r_∞ is the limiting anisotropy for the hindered motion, and θ is the molecule rotational correlation time. If we define fluorescence joint time ξ

$$\frac{1}{\xi} = \frac{1}{\tau} + \frac{1}{\theta}, \tag{6}$$

Equations 4 and 5 forms the system of the linear equations of two unknowns: parallel component I_{II} (t) and perpendicular component $I_\perp(t)$. After replacing the relevant values in the system equations by Eq. 6, their roots may be rewritten as,

$$\begin{aligned} I_{\mathrm{II}}(t) &= \frac{1}{3} \cdot [2r(t) \cdot I(t) + I(t)] \\ &= \frac{I_0}{3} \cdot [2(r_0 - r_\infty) \cdot \exp(-t/\xi) + (1 + 2r_\infty) \cdot \exp(-t/\tau)], \end{aligned} \tag{7}$$

$$\begin{aligned} I_\perp(t) &= \frac{1}{3} \cdot [I(t) - r(t) \cdot I(t)] \\ &= \frac{I_0}{3} \cdot [(1 - r_\infty) \cdot \exp(-t/\tau) - (r_0 - r_\infty) \cdot \exp(-t/\xi)]. \end{aligned} \tag{8}$$

If $r_0 = r_\infty = 0.4$, then

$$I_{\mathrm{II}}(t) = 0.6 \cdot I_0 \cdot \exp(-t/\tau), \tag{9}$$

$$I_\perp(t) = 0.2 \cdot I_0 \cdot \exp(-t/\tau). \tag{10}$$

Therefore, in the phasor space, $I_{\mathrm{II}}(t)$, $I_\perp(t)$ and $I(t)$ are completely overlapped and represented by the only one point located on the semicircle.

Unfortunately, Eq. 7 is different from Eq. 6 in [15]. At first, the first term inside the square brackets in the Eq. 6 in [15] is $(2r_0 - r_\infty)$ exp(...), however, the comparable term in the Eq. 7 above is $2(r_0 - r_\infty)$ exp (...). Secondly, A. H. A. Clayton didn't give out the details how his Eq. 6 was deduced. Thirdly, if $r_0 = r_\infty = 0.4$, we can find that $I(t)$ and $I_\perp(t)$ in A. H. A. Clayton's paper are not overlapped in the phasor space, shown in his Fig. 2(b) [15]. this is contradictory to our conclusion in the Eq. 9, 10. These hint that the difference between Eq. 7 in this paper and Eq. 6 in

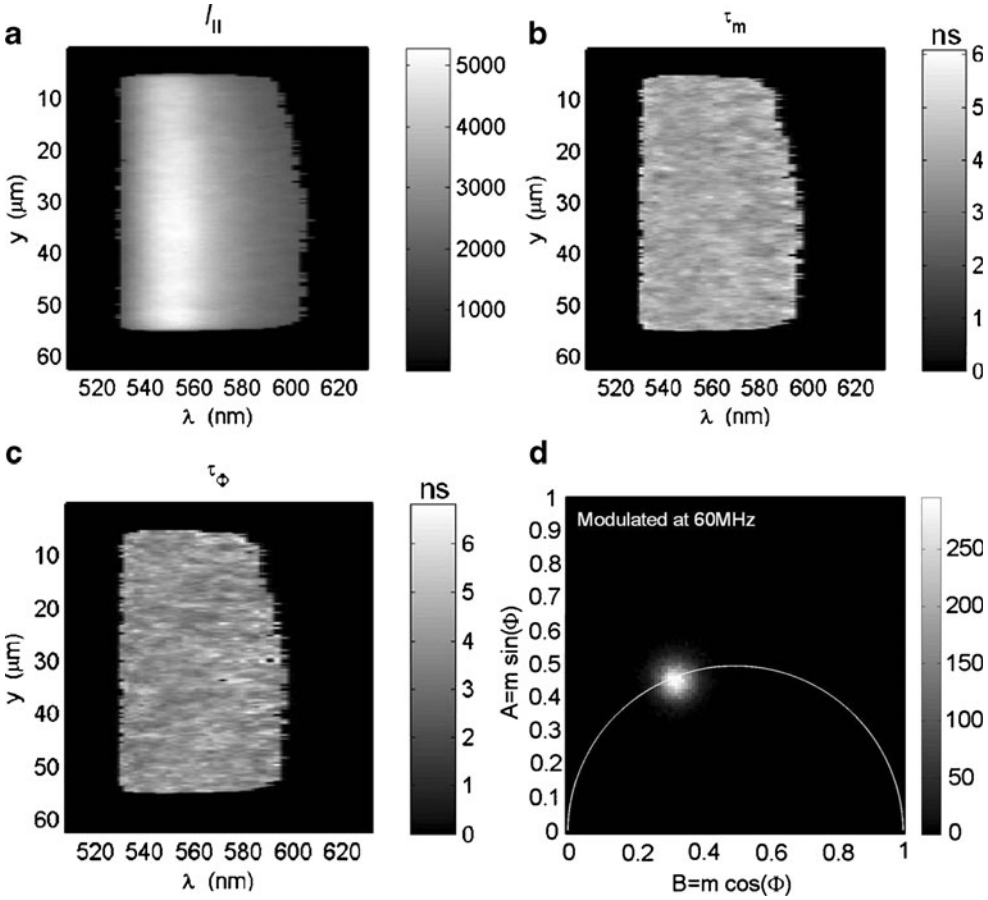

Fig. 1 Experimental results for 10 μM rhodamine 6G solutions mixed with 74% glycerol and deionized water, **a** spectrum of the parallel polarization component; spectrum of the fluorescence lifetime calculated from, **b** modulation depth m; **c** phase shift φ; **d** phasor histogram of the fluorescence lifetime

[15] is not a typo, and this matter needs to be spelt out for the reader.

After subtracting of Eq. 8 from Eq. 7, we obtain

$$\begin{aligned}\Delta I(t) &= I_{\mathrm{II}}(t) - I_{\perp}(t) = r(t)\cdot I(t)\\ &= I_0\cdot[(r_0 - r_\infty)\cdot\exp(-t/\xi) + r_\infty\cdot\exp(-t/\tau)],\end{aligned} \tag{11}$$

If $r_\infty = 0$, the parallel and perpendicular light intensities take the forms of,

$$\begin{aligned}I_{\mathrm{II}}(t) &= \tfrac{I_0}{3}\cdot[2r_0\cdot\exp(-t/\xi) + \exp(-t/\tau)],\\ I_{\perp}(t) &= \tfrac{I_0}{3}\cdot[\exp(-t/\tau) - r_0\cdot\exp(-t/\xi)].\end{aligned} \tag{12}$$

Furthermore,

$$\Delta I(t) = I_{\mathrm{II}}(t) - I_{\perp}(t) = I_0\cdot r_0\cdot\exp(-t/\xi). \tag{13}$$

$^{\triangle}I(t)$ is a single exponential decay with the time constant ξ defined at Eq. 6, which is represented by a point on the semicircle in the phasor space.

By the linearly interpolation and extrapolation between the points mapped from the two single exponential lifetimes ξ and τ in the phasor space, $I_{\mathrm{II}}(t)$ and $I_{\perp}(t)$ are denoted by the points inside and outside the semicircle, respectively, which are asymmetrically distributed around the point representing the lifetime τ. $I_{\mathrm{II}}(t)$ is a little bit far from the semicircle, and $I_{\perp}(t)$ is a little bit close to the semicircle. In the histograms, it is difficult to distinguish $I(t)$ from $I_{\perp}(t)$, meanwhile, even though $I_{\mathrm{II}}(t)$ is a little bit far from $I(t)$ in the phasor plot, in some case, for example, $r_0 \to 0.4$, $\xi \to \tau$, it is very difficult to distinguish $I(t)$ from $I_{\mathrm{II}}(t)$ also.

In order to verify the approach, we use the experimental results collected with the fluorescence spectral lifetime and anisotropy imaging microscopy in the frequency domain (rsFLIM) [12]. After transforming the time-resolved fluorescence parallel, perpendicular components and light intensity at each pixel into the phasor space, a series of the phasor histograms are given out, in terms of Eqs. 4, 12 and 13.

To validate the accuracy of the rsFLIM, experimental data were obtained from 10 μM rhodamine 6G solutions mixed with 0%, 15%, 37%, 45%, 59%, 74% and 91% glycerol and deionized water at the light modulated frequency 60 MHz. The varying refractive indexes of the glycerol solutions are shown to adjust the fluorescence lifetime of rhodamine 6G slightly. A Strickler–Berg plot of $1/\tau$ versus the square of the refractive index follow the expected straight line and are in good agreement with previous results [12] Fig. 1.

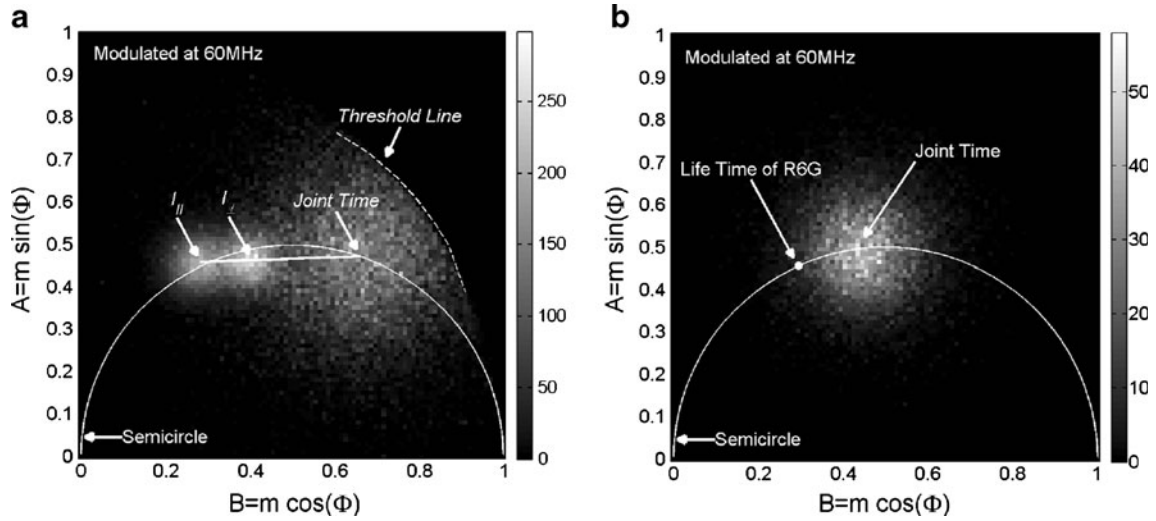

Fig. 2 Polarized phasor histograms of the fluorescence lifetime and joint time of 10 μM rhodamine 6G solutions mixed with, **a** 74% glycerol, where the histogram data of the fluorescence joint time is multiplied by 10; **b** 91% glycerol. The measured data should be located within a threshold curve (dash) ($m \leq 1$). The formula of the threshold curve is $m=1$, or $B = \cos\phi$ and $A = \sin\phi$

The wavelength-resolved experimental data from 10 μM rhodamine 6G solutions mixed with 74% glycerol solution are shown in the Fig. 1(a) to (c). After every pixels in the spectrum of the fluorescence lifetime (see Fig. 1(b) (c)) is mapped to the phasor space, according to Eqs. 1 and 4, the histogram distribution of the fluorescent lifetime in the phasor space is shown in the Fig. 1(d). It is a circular Gaussian distribution with its center located on the semicircle, means that the fluorescence processing is a single exponential decay. Therefore, we conclude that the rsFLIM system works in the good condition.

The phasor histograms of the fluorescence joint times of 10 μM rhodamine 6G solutions mixed with 74%, 91% glycerol are shown in the Fig. 2(a) (b), respectively. The fluorescence joint times are 1.81 ns, 2.84 ns and the rotational correlation times are 3.42 ns, 12.51 ns, respectively. A. H. A Clayton reported that his method is expected to be sensitive to noise [15]. In this paper, we find the similar phenomenon that the phasor plot of the fluorescence joint time is noisier than that of the fluorescence lifetime (see Fig. 2(a) (b) and Fig. 1 (d)). It should be noted that this noise doesn't come from the modeling of Eqs. 11 or 13, but inherits from the dynamic anisotropy itself, and is independent to model. This noise should be paid more attention.

In the Fig. 2(a), we draw the histograms of the fluorescence lifetimes of the parallel and perpendicular components and the fluorescence joint time on the same plot, and find that the centre of the parallel polarized light is located inside the semicircle, perpendicular one outside the semicircle and the centre of the joint time is on the semicircle. All of these three points are located on a straight line in the phasor space, which is first described by A. H. W. Clayton [15], validated by Eq. 13 in this paper. However, shown in Fig. 2(b), as the fluorescence times $I_{\mathrm{II}}(t)$ and $I_{\perp}(t)$ are close to each other, the linear extrapolation to determine the fluorescence joint time turns out to be an ill-posed mathematical problem, and any tiny interference on $I_{\mathrm{II}}(t)$ and $I_{\perp}(t)$ often produces intolerant errors; therefore, drawing the histogram of the fluorescence joint time directly in terms of Eq. 13 has advantage by birth. As much as the biosamples such as the fluorescence proteins are concerned, none of the histograms of the parallel and perpendicular components, light intensity and dynamic anisotropy in the phasor space are circular Gauss distribution, and it is impossible to find their centers for interpolating and extrapolating a straight line point to the fluorescence joint time, therefore, it is particularly valuable to give out the phasor histograms of the fluorescence joint time directly using Eqs. 7, 8, 11, 13 for the global analysis of the biological samples.

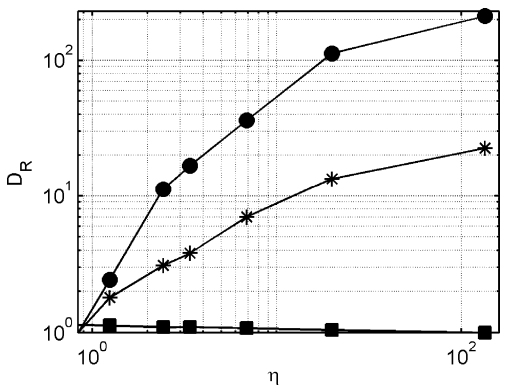

Fig. 3 Dynamic ranges (D_{R}) of ■ normalized lifetime $D_{\mathrm{R}} = \tau / \min(\tau)$; *normalized steady state anisotropy $D_{\mathrm{R}} = r_{\mathrm{DC}} / \min(r_{\mathrm{DC}})$; ● normalized joint time $D_{\mathrm{R}} = \xi / \min(\xi)$

The fluorescence dynamic anisotropy can be evaluated by the parameters—steady state anisotropy r_{DC}, dynamic anisotropy r_{AC}, phase shift between parallel and perpendicular components $^{\triangle}\varphi$, rotational correlation time θ [10, 12], and a new parameter-the fluorescence joint time ξ, which we put forward in this paper. Both r_{DC} and r_{AC} are nonlinear proportional to the local viscosity and approach to an asymptote r=0.4 [12, 13]. $^{\triangle}\varphi$ shows a single hump response to the local viscosity, and as η>10, it decreases. The rotational correlation time related to r_{DC}, r_{AC} and $^{\triangle}\varphi$ is not an independent parameter, and proportional to the viscosity η with a ratio 0.108, conformed to the relation $\theta = \eta V/RT$ [13]; up to now, it is impossible to draw the phasor plot of the rotational correlation time in the phasor space. It should be realized that the parameters above may not be immediate informative for the evaluation of any fluorescence processing, for the data from each pixel of the imaging represents a compound measurement over multiple molecules and fluorescence cycles [7, 19]. r_{DC} , r_{AC} and $^{\triangle}\varphi$ exhibit the information on average, and cannot be used to extract the fractions of the multiple fluorescence processing. Among the parameters of the fluorescence dynamic anisotropy, only fluorescence joint time ξ has a relatively larger dynamic range than that of the fluorescence lifetime (see Fig. 3) and can be transformed to the phasor space, that is particularly useful to distinguish multiple fluorescence cycles using the concept of trajectories and mapping between the phasor space and intensity imaging [7, 19]. In the end, we reach a conclusion that fluorescence joint time ξ is the most suitable parameter to weigh macromolecule dynamics.

Acknowledgement This work was partially supported by the Engineering and Physical Sciences Research Council,U.K. under a Life Science Interface Grant EP/E013422/1, and is supported now by State 211 Project, P. R. China, under Grant YueFaGai 2009 (432). The author is grateful to Dr. Q. S. Hanley of Nottingham Trent University, U.K. for his encouragement and helpful discussions.

References

1. Jameson DM, Gratton E, Hall RD (1984) The measurement and analysis of heterogeneous emissions by multifrequency phase and modulation fluorometry. Appl Spectrosc Rev 20:55–106
2. Clayton AHA, Hanley QS, Verveer PJ (2004) Graphical representation and multicomponent analysis of single-frequency fluorescence lifetime imaging microscopy data. J Microsc 213:1–5
3. Verveer PJ, Bastiaens PIH (2003) Evaluation of global analysis algorithms for single frequency fluorescence lifetime imaging microscopy data. J Microsc 209:1–7
4. Hanley QS, Clayton AHA (2005) AB-plot assisted determination of fluorophore mixtures in a fluorescence lifetime microscope using spectra or quenchers. J Microsc 218:62–67
5. Hanley QS (2009) Spectrally resolved fluorescent lifetime imaging. J R Soc Interface 6:S83–S92
6. Grecco HE, Roda-Navarro P, Verveer PJ (2009) Global analysis of time correlated single photon counting FRET-FLIM data. Opt Express 17:6493–6508
7. Digman MA, Caiolfa VR, Zamai M, Gratton E (2008) The phasor approach to fluorescence lifetime imaging analysis. Biophys J 94: L14–L16
8. Redford GI, Clegg RM (2005) Polar plot representation for frequency-domain analysis of fluorescence lifetimes. J Fluoresc 15:805–815
9. Verveer PJ, Squire A, Bastiaens PIH (2000) Global analysis of fluorescence lifetime imaging microscopy data. Biophys J 78:2127–2137
10. Clayton AHA, Hanley QS, Arndt-Jovin DJ, Subramaniam V, Jovin TM (2002) Dynamic fluorescence anisotropy imaging microscopy in the frequency domain (rFLIM). Biophys J 83:1631–1649
11. Jares-Erijman EA, Jovin TM (2003) FRET imaging. Nat Biotechnol 21:1387–1395
12. Zhou Y, Dickenson JM, Hanley QS (2009) Imaging lifetime and anisotropy spectra in the frequency domain. J Microsc 234:80–88
13. Lakowicz JR (2006) Principles of fluorescence spectroscopy, 3rd edn. Springer, New York
14. Suhling K, Siegel J, Lanigan PMP, Leveque-Fort S, Webb SED, Phillips D, Davis DM, French PMW (2004) Time-resolved fluorescence anisotropy imaging applied to live cells. Opt Lett 29:584–586
15. Clayton AHA (2008) The polarized AB plot for the frequency-domain analysis and representation of fluorophore rotation and resonance energy homotransfer. J Microsc 232:306–312
16. Siegel J, Suhling K, Leveque-Fort S, Webb SED, Davis DM, Phillips D, Sabharwal Y, French PMW (2003) Wide-field time-resolved fluorescence anisotropy imaging (TR-FAIM): Imaging the rotational mobility of a fluorophore. Rev Sci Instrum 74:182–192
17. Lakowicz JR, Balter A (1982) Analysis of excited-state processes by phase-modulation fluorescence spectroscopy. Biophys Chem 16:117–132
18. Lakowicz JR, Balter A (1982) Theory of phase-modulation fluorescence spectroscopy for excited-state processes. Biophys Chem 16:99–115
19. Wouters FS, Esposito A (2008) Quantitative analysis of fluorescence lifetime imaging made easy. Journal of HFSP 2:7–11